A Model of the Quaternary Structure of the *Escherichia coli* F_1 ATPase from X-Ray Solution Scattering and Evidence for Structural Changes in the Delta Subunit during ATP Hydrolysis

Dmitri I. Svergun,[*#] Ingo Aldag,[§] Tanja Sieck,[§] Karlheinz Altendorf,[§] Michel H. J. Koch,[*] David J. Kane,[¶] Michael B. Kozin,[#‖] and Gerhard Grüber[§]

[*]European Molecular Biology Laboratory, Hamburg Outstation, D-22603 Hamburg, Germany; [#]Institute of Crystallography, Russian Academy of Sciences, 117333 Moscow, Russia; [§]Universität Osnabrück, Fachbereich Biologie/Chemie, D-49069 Osnabrück, Germany; [¶]Department of Biophysical Chemistry, Max-Planck-Institut für Biophysik, D-60596 Frankfurt am Main, Germany; and [‖]GKSS Research Center, GKSS-WS, D-21502 Geesthacht, Germany

ABSTRACT The shape and subunit arrangement of the *Escherichia coli* F_1 ATPase (*EC*F_1 ATPase) was investigated by synchrotron radiation x-ray solution scattering. The radius of gyration and the maximum dimension of the enzyme complex are 4.61 ± 0.03 nm and 15.5 ± 0.05 nm, respectively. The shape of the complex was determined ab initio from the scattering data at a resolution of 3 nm, which allowed unequivocal identification of the volume occupied by the $\alpha_3\beta_3$ subassembly and further positioning of the atomic models of the smaller subunits. The δ subunit was positioned near the bottom of the $\alpha_3\beta_3$ hexamer in a location consistent with a β–δ disulfide formation in the mutant *EC*F_1 ATPase, βY331W:βY381C:ϵS108C, when MgADP is bound to the enzyme. The position and orientation of the ϵ subunit were found by interactively fitting the solution scattering data to maintain connection of the two-helix hairpin with the $\alpha_3\beta_3$ complex and binding of the β-sandwich domain to the γ subunit. Nucleotide-dependent changes of the δ subunit were investigated by stopped-flow fluorescence technique at 12°C using *N*-[4-[7-(dimethylamino)-4-methyl]coumarin-3-yl]maleimide (CM) as a label. Fluorescence quenching monitored after addition of MgATP was rapid [$k = 6.6\ s^{-1}$] and then remained constant. Binding of MgADP and the noncleavable nucleotide analog AMP · PNP caused an initial fluorescent quenching followed by a slower decay back to the original level. This suggests that the δ subunit undergoes conformational changes and/or rearrangements in the *EC*F_1 ATPase during ATP hydrolysis.

INTRODUCTION

The membrane-integrated ATP synthase of *Escherichia coli* (*EC*F_1F_O) consists of an extrinsic F_1 domain, containing the catalytic sites for reversible ATP synthesis and hydrolysis, and the intrinsic F_O domain, which is involved in proton translocation. *EC*F_O consists of three different subunits, designated *a*, *b*, and *c* in the stoichiometry ab_2c_{9-12}. The *EC*F_1 complex (~380 kDa) contains five subunits in the stoichiometry $\alpha_3\beta_3\gamma\delta\epsilon$ (Engelbrecht and Junge, 1997; Deckers-Hebestreit and Altendorf, 1996).

The F_1 ATPase has been crystallized (Bianchet et al., 1991; Abrahams et al., 1994; Shirakihara et al., 1997; Grüber et al., 1997) and most information has been obtained from the structure of the bovine heart mitochondrial F_1 (MF_1) at 0.28 nm resolution (Abrahams et al., 1994). This structure reveals the α and β subunits alternating in an almost symmetrical arrangement around the γ subunit. Approximately half of the γ subunit resolved in the structure is arranged in three α-helices. Other portions of the γ subunit and the δ and ϵ subunits are unresolved, presumably due to disorder in the crystal.

The structure of the ϵ subunit (*EC*F_1), which is composed of a C-terminal helix-loop-helix domain and an N-terminal domain, arranged as a β sandwich with two five-stranded sheets, has been determined by NMR and x-ray crystallography (Wilkens et al., 1995; Uhlin et al., 1997). Detailed structural features of the N-terminal domain (residues 1–134) of the δ subunit (*EC*F_1), which are currently being determined by NMR, suggest a bundle of 6 α-helices forming an α-barrel (Wilkens et al., 1996).

Knowledge of the arrangements of the domains is essential for any proposed molecular mechanism in the F_1 ATPase complex. The shape and dimensions of the chloroplast F_1 (CF_1) and *EC*F_1 have been studied by electron microscopy (Boekema and Böttcher, 1992; Gogol et al., 1989a) and cryoelectron microscopy (Gogol et al., 1989b).

Solution scattering allows the determination of the overall structures of native biological macromolecules under nearly physiological conditions (Feigin and Svergun, 1987). Recently, techniques for the interpretation of solution scattering data in terms of spherical harmonics were further developed (Svergun and Stuhrmann, 1991; Svergun, 1994; Svergun et al., 1996) and successfully applied to study the quaternary structure of biopolymers in solution (Svergun et al., 1997a, b). Here we present a model of the *EC*F_1 ATPase that integrates the crystallographic models of the $\alpha_3\beta_3$ subcomplex (Abrahams et al., 1994) and the ϵ subunit (Uhlin et

Received for publication 23 March 1998 and in final form 11 August 1998.

Address reprint requests to Dr. Gerhard Grüber, Universität Osnabrück, Fachbereich Biologie/Chemie, D-49069 Osnabrück, Germany. Tel.: +49-541-969-2809; Fax: +49-541-969-2870; E-mail: grueber@sfbbio1.biologie.uni-osnabrueck.de.

Abbreviations used: *EC*F_1F_O, *Escherichia coli* F_1F_O ATP synthase; CM, *N*-[4-[7-(dimethylamino)-4-methyl]coumarin-3-yl)]maleimide; *EC*F_1, soluble portion of the *Escherichia coli* F_1F_O ATP synthase; PAGE, polyacrylamide gel electrophoresis.

0006-3495/98/11/2212/08 $2.00

al., 1997), as well as the NMR model of the N-terminal domain of the δ subunit (Wilkens et al., 1996) into the shape of the complex obtained ab initio from the x-ray solution scattering data. The relative positions of the minor subunits in the model are supported by cross-linking and fluorescence studies.

MATERIALS AND METHODS

Scattering experiments and data treatment

X-ray scattering data were collected using standard procedures on the X33 camera (Koch and Bordas, 1983; Boulin et al., 1986, 1988) of the EMBL on the storage ring DORIS III of the Deutsches Elektronen Synchrotron (DESY) and multiwire proportional chambers with delay line readout (Gabriel and Dauvergne, 1982). At a sample-detector distance of 4.4 m and a wavelength $\lambda = 0.15$ nm, the range of momentum transfer $0.12 < s < 1.6$ nm^{-1} was covered ($s = 4\pi \sin\theta/\lambda$, where 2θ is the scattering angle). The data were normalized to the intensity of the incident beam, corrected for the detector response, the scattering of the buffer was subtracted, and the difference curves were scaled for concentration using the program SAPOKO (Svergun and Koch, unpublished data).

The invariants (maximum dimension, forward scattering, radius of gyration) were evaluated using the orthogonal expansion program ORTOGNOM (Svergun, 1993) and the indirect transform program GNOM (Svergun et al., 1988; Svergun, 1992).

Shape determination

The low resolution particle envelope was determined from the experimental data following an ab initio procedure (Svergun and Stuhrmann, 1991; Svergun, 1994; Svergun et al., 1996). The particle shape is represented by an angular envelope function $F(\omega)$, where $\omega = (\theta, \varphi)$ are spherical coordinates, which is parametrized as (Stuhrmann, 1970)

$$F(\omega) = \sum_{l=0}^{L} \sum_{m=-l}^{l} f_{lm} Y_{lm}(\omega) \qquad (1)$$

where f_{lm} are complex numbers and $Y_{lm}(\omega)$ are spherical harmonics. The resolution of this representation is equal to $\delta r = \pi R_0/(L + 1)$, where R_0 is the radius of the equivalent sphere. The scattering intensity of the envelope is evaluated as

$$I(s) = 2\pi^2 \sum_{l=0}^{\infty} \sum_{m=-l}^{l} |A_{lm}(s)|^2, \qquad (2)$$

where the partial amplitudes $A_{lm}(s)$ are calculated from the coefficients f_{lm} using a recurrence relation (Svergun and Stuhrmann, 1991). The algorithms for rapid evaluation of $I(s)$ taking into account the particle-solvent interface are described elsewhere (Svergun et al., 1996, 1997c). The shape was determined using terms up to $L = 5$ and assuming a threefold symmetry of the molecule that yields 11 free parameters f_{lm} in Eq. 1. Starting from a sphere as the initial approximation, these parameters were obtained by using a nonlinear optimization procedure by minimizing the discrepancy

$$\chi^2 = \frac{1}{N-1} \sum_{j=1}^{N} \left[\frac{I(s_j) - I_{exp}(s_j)}{\sigma(s_j)} \right]^2 \qquad (3)$$

where N is a number of experimental points and $I_{exp}(s)$ and $\sigma(s)$ denote the experimental intensity and its standard deviation, respectively.

To position the ε subunit within the low resolution envelope, scattering amplitudes from the $\alpha_3\beta_3\gamma$ subassembly together with the δ subunit and ε domain were evaluated using the crystallographic and NMR coordinates in the Brookhaven Protein Data Bank (Bernstein et al., 1977), entries 1bmf (Abrahams et al., 1994), 1abv (Wilkens et al., 1996), and 1aqt (Uhlin et al., 1997), respectively. The program CRYSOL, used to compute the amplitudes, also takes the scattering from the solvation shell into account (Svergun et al., 1995). The scattering intensity from a complex between the assembly and an arbitrarily positioned ε subunit was evaluated as follows: given the amplitudes of the two particles in reference positions, denoted as $A_1(s)$ and $A_2(s)$, respectively, and assuming that the $\alpha_3\beta_3\gamma\delta$ assembly is fixed while the ε subunit is rotated and moved, one obtains

$$I(s) = I_1(s) + I_2(s) + 2\langle A_1(\mathbf{s}) \prod [A_2^*(\mathbf{s}, \mathbf{u})] \rangle_\Omega \qquad (4)$$

where $I_1(s)$ and $I_2(s)$ are the scattering intensities of the two particles. Here, Π describes the rotation over the three Euler angles, **u** is the translation, Ω is the solid angle in reciprocal space, and $s = (s, \Omega)$ is the momentum transfer vector. The amplitudes of a shifted ε subunit, $A_2(\mathbf{s}, \mathbf{u})$, required to compute the third (cross) term in Eq. 4 are rapidly evaluated using the multipole expansion method (Svergun, 1994). The six positional parameters of the ε subunit were determined to minimize the discrepancy in Eq. 3 using the interactive graphical software package *ASSA* (Kozin et al., 1997), which permits three-dimensional display and manipulation of low resolution and atomic models, coupled with the intensity evaluation program *ALM22INT* (Svergun and Kozin, unpublished data).

Fluorescence measurements

Before labeling with CM, *EC*F_1 ATPase was depleted of nucleotides as described below. The enzyme was labeled with 20 μM CM for 20 min in the dark before the reaction was stopped with L-Cys (20 mM). Excess label was removed by one pass through a Sephadex G-25 spin column, equilibrated in 50 mM MOPS, pH 7.5, and 10% glycerol (v/v) (Turina and Capaldi, 1994).

Steady-state measurements were recorded with a Hitachi F-4500 fluorescence spectrophotometer. The volume of the sample was 500 μl in a 0.4 × 1 cm quartz cuvette. Fluorescence emission spectra of CM-bound *EC*F_1 ATPase were performed with an excitation wavelength of 365 nm at 12°C.

Stopped-flow experiments were performed using an SF-61 stopped-flow spectrofluorimeter from Hi-Tech Scientific Ltd. (Salisbury, UK). The solution in the observation chamber was excited using a 100 W short arc mercury lamp (Osram, Frankfurt, Germany), and the fluorescence was detected at right angles to the incident light beam using an R928 multialkali side-on photomultiplier. All reactions were performed in 50 mM MOPS, pH 7.5, and 10% glycerol (v/v) at 12°C using an excitation wavelength of 365.1 nm and a cutoff filter (420 nm; Schott, Mainz, Germany) in front of the photomultiplier. The kinetic data were collected by a high-speed 12-bit analog-to-digital data acquisition board and were analyzed using software developed by Hi-Tech Scientific LTD (Salisbury, UK). Each individual kinetic trace consisted of 1024 data points. Typically, between 5 and 12 experimental traces were averaged.

Other methods

The *EC*F_1 mutant βY331W:βE381C:εS108C was obtained from the strain RA1 (Aggeler et al., 1997) containing plasmid pGG1 (Grüber and Capaldi, 1996a). The purification of F_1 ATPase was accomplished as previously described (Grüber et al., 1997). *EC*F_1 isolated according to this method is heterogeneous with respect to the nucleotide content of both catalytic and noncatalytic sites. Thus, bound nucleotides were removed by precipitation with 70% ammonium sulfate and three consecutive spin columns (Sephadex G-50 medium), which were equilibrated in 50 mM MOPS, pH 7.5, 0.5 mM EDTA, and 10% glycerol (v/v). After this treatment *EC*F_1 preparations retained residual amounts of bound nucleotide [0.1–0.3 mol/ATP/mole enzyme (Grüber et al., 1997)]. Homogeneity of protein samples was

tested by $NaDodSO_4$-polyacrylamide gel electrophoresis according to Schägger and von Jagow (1987). Cross-linking between subunits was induced by $CuCl_2$, as described by Aggeler et al. (1995). Protein concentrations were determined according to Dulley and Gieve (1975). ATP hydrolysis was measured as described by Fiske and Subbarow (1925) with a continuous analysis system (Arnold et al., 1976).

RESULTS

The x-ray scattering curve for the wild-type $EC F_1$ ATPase at saturating MgATP concentrations, followed by turnover of the enzyme, is presented in Fig. 1. The maximum dimensions of the particle (D_{max}) and radius of gyration (R_g) are 16.0 ± 0.5 nm and 4.61 ± 0.03 nm, respectively. Comparison of the normalized forward scattering with the values obtained for a reference solution of bovine serum albumin yields 390 ± 20 kDa, in agreement with that expected from the chemical composition of the $EC F_1$ ATPase. This indicates that aggregation of the enzyme complex at the concentrations used does not occur. Exposure to x-rays had no influence on the hydrolytic activity (11 μmol ATP hydrolyzed · mg^{-1} · min^{-1}) of the enzyme.

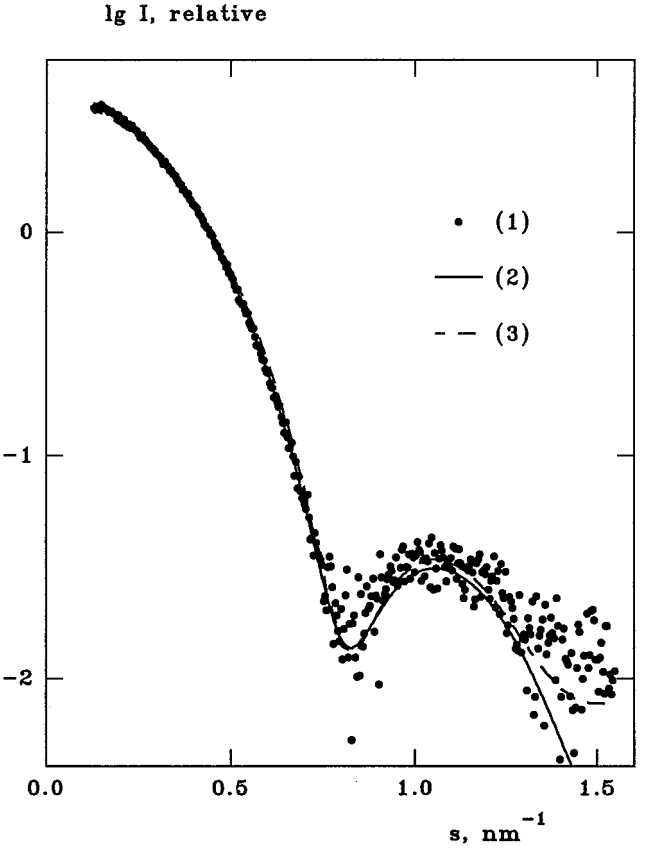

FIGURE 1 Experimental scattering curve from the wild-type $EC F_1$ ATPase (*1*), the curves calculated from the low resolution shape (*2*), and from the subunits positioned as in Fig. 2 (*3*). The x-ray scattering of the $EC F_1$ ATPase (10 mg/ml) was measured after incubation (10 min) of the nucleotide free enzyme with 2 mM MgATP (ratio of 1:1) at room temperature.

The particle envelope restored ab initio at a resolution of 3 nm, as described in Materials and Methods, is shown in Fig. 2 and fitted to the experimental data with $\chi = 0.86$ (Fig. 1). The central part of the low resolution model has a pronounced threefold symmetry and can be unequivocally identified as the $\alpha_3\beta_3$ subassembly. Space for the γ, δ, and ϵ subunits remains in a protuberance along the threefold axis. The envelope in Fig. 2 thus provides the first direct experimental evidence for the quaternary structure of the $EC F_1$ ATPase in solution.

The known atomic models of the subunits were positioned inside the low resolution model. The crystallographic model of the $\alpha_3\beta_3$ subassembly (Abrahams et al., 1994) is well accommodated within the central part, and its orientation along the threefold axis is uniquely selected to position the α-helical domain of the γ subunit in the protuberance of the shape. The smaller subunits were positioned with respect to the $\alpha_3\beta_3$ moiety and the α-helical domain of the γ subunit using the graphical package *ASSA*, as described in Materials and Methods. The discrepancy between the experimental and calculated scattering curves was minimized interactively to keep the subunits within the low resolution envelope of the entire enzyme. The solution providing the best fit is shown in Fig. 2 with $\chi = 1.68$ (Fig. 1). The model indicates the δ subunit near the bottom of the $\alpha_3\beta_3$ complex and at the interface of an $\alpha\beta$ pair. Positioning of the δ subunit at the top of the $EC F_1$ ATPase correlates with higher χ values. The C-terminal domain of the ϵ subunit lies under the C-terminal part of one of the β subunits. The 10-stranded β barrel is close to the α-helical domain of the γ subunit.

To further examine the position of the δ subunit, the recently described $EC F_1$ mutant βY331W:βE381C:ϵS108C (Grüber and Capaldi, 1996b) was used. When $EC F_1$ from the mutant βY331W:βE381C:ϵS108C was reacted with $CuCl_2$ after addition of ATP + Mg^{2+}, followed by the turnover of the enzyme, disulfide bond formations between $\beta + \gamma$, $\beta + \epsilon$, $\beta + \delta$, and $\alpha + \delta$ were formed in essentially full yield (Fig. 3 *A*). Previous work (Bragg and Hou, 1986; Tozer and Dunn, 1986; Mendel-Hartvig and Capaldi, 1991) has shown that an $\alpha + \delta$ cross-linked product can be generated by passage of the $EC F_1$ ATPase through spin columns, which are used for removing bound nucleotides. The data in Fig. 3 *B* confirm that an $\alpha + \delta$ cross-link is obtained when $CuCl_2$ was used to induce disulfide bond formation, showing that there are two structural arrangements and/or conformations in the $EC F_1$ ATPase, one found when nucleotides have been removed and the second one when ADP is present in the catalytic sites.

To explore these structural changes we have specifically labeled Cys^{140} of the δ subunit (Ziegler et al., 1994) using the fluorescent label CM, as visualized on the polyacrylamide gel in Fig. 4, and looked for nucleotide-dependent fluorescence changes. Fig. 5 shows the fluorescence spectrum of the CM labeled $EC F_1$ ATPase, which was freed of tightly bound nucleotides by passage through three Sephadex columns. For comparison, a spectrum of enzyme from

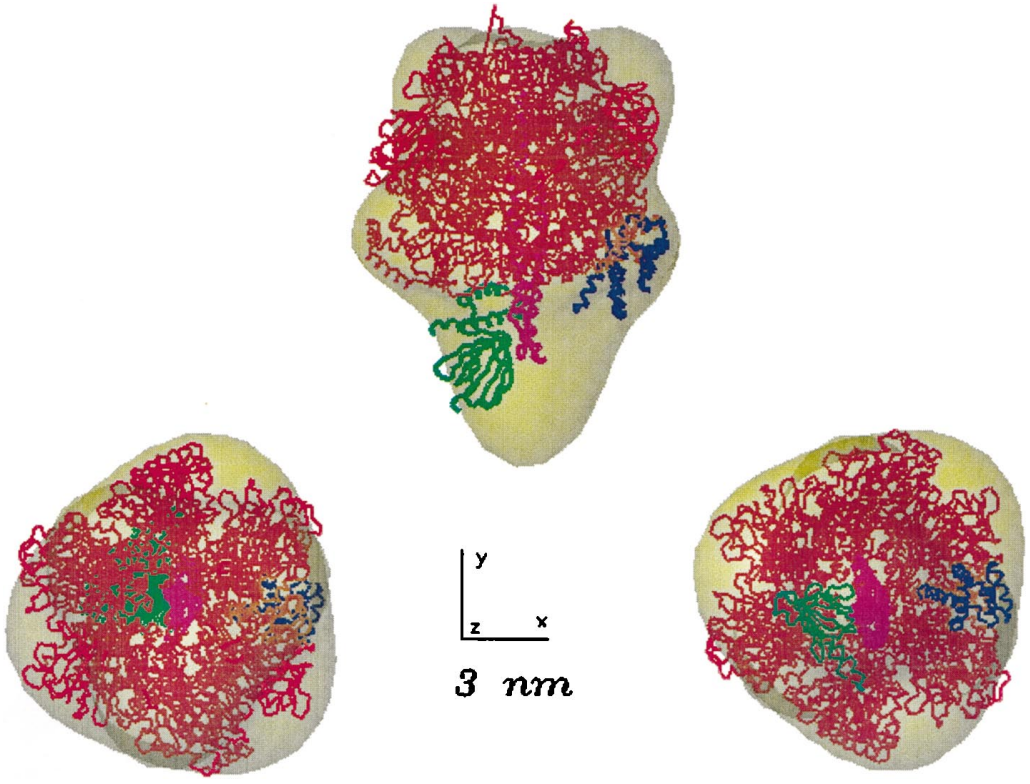

FIGURE 2 Low resolution envelope of the *EC*F_1 ATPase derived from scattering data (semitransparent envelope) and its constructed model. The atomic structure of the $\alpha_3\beta_3$ complex is shown in red, that of the γ subunit [γ1–45, γ73–90, and γ209–272 (Abrahams et al., 1994)] in magenta, the ϵ subunit (Uhlin et al., 1997) in green, and the NMR structure of the N-terminal domain of the δ subunit (Wilkens et al., 1996) in blue.

which nucleotides have been removed before titration of MgATP (in a 1:1 ratio; *curve 1*) is presented. The addition of MgATP to the protein causes the signal to increase and to shift to longer wavelengths (*curve 2*). Importantly, addition of MgADP (*curve 4*) and the noncleavable nucleotide analog AMP · PNP (*curve 3*) resulted in a decrease of fluorescence intensity and a shift to shorter wavelengths. These findings indicate that the fluorescence spectrum of CM bound to the δ subunit is sensitive to nucleotide binding. To examine these conformational changes more precisely, the kinetics of the fluorescence changes were compared with those of ATP hydrolysis. The nucleotide-depleted *EC*F_1 ATPase was rapidly mixed with MgATP (final concentration 2 mM) at 12°C by using the stopped-flow technique. A typical transient is shown in Fig. 6. The reduction in fluorescence after mixing with MgATP could confidently be fitted to a monoexponential time function (*curve C*), with a rate constant of 6.6 s^{-1}, similar to the rate (k = 7.2 s^{-1}) of ATP hydrolysis at 12°C (T. Sieck, K. Altendorf, and G. Grüber, unpublished data). For comparison, addition of MgAMP · PNP resulted in a rapid decrease in fluorescence, followed by a slower increase (*curve A*). Addition of MgADP (*curve B*) causes a transient similar to that observed with the noncleavable nucleotide analog AMP · PNP. These results indicate that ATP hydrolysis and the structural changes and/or rearrangements of the δ subunit described above are sensitive to nucleotide binding.

DISCUSSION

X-ray solution scattering was used to investigate the quaternary structure and subunit arrangement of the *EC*F_1 ATPase at saturating nucleotide conditions. The shape of the native enzyme was derived from the experimental data assuming threefold symmetry for the entire molecule, which is justified given that the major part of the ATPase, its $\alpha_3\beta_3$ subassembly, possesses a quasi-threefold symmetry. The symmetry restriction results in a significant reduction in the number of free parameters in the model (without symmetry, description of the particle envelope up to L = 5 would have required 30 independent parameters instead of 11). Shape determination is unique when the number of independent parameters in the model M does not exceed 1.5 times the number of Shannon channels in the experimental data $N_s = D_{max}s_{max}/\pi$ (Svergun et al., 1996). In the present case, N_s = 8 and M = 11, so the low resolution symmetric model in Fig. 2 can be considered to be unique. The asymmetry, as described particularly in the nucleotide occupancy and the conformations of the β subunits of the high resolution structure of the $\alpha_3\beta_3\gamma$ subcomplex, crystallized under subsaturating amounts of Mg AMP · PNP and MgADP (Abrahams et al., 1994), cannot be meaningfully analyzed at low resolution. Although small deviations from the ideal symmetry might be described with a few additional parameters only, the scattering data would not be sufficiently sensitive

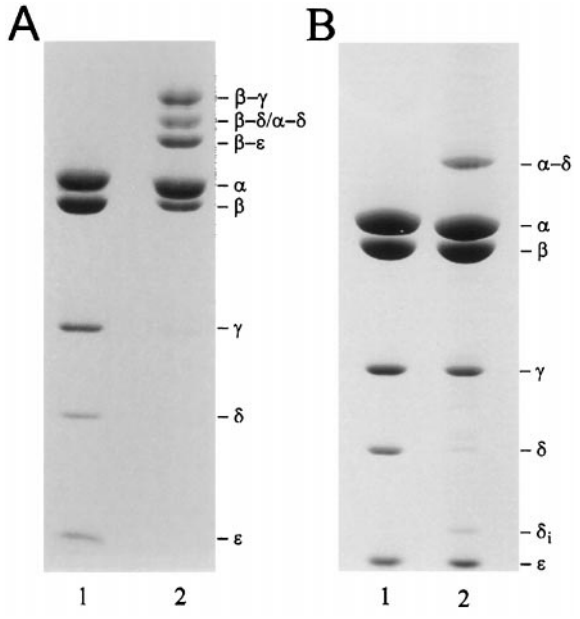

FIGURE 3 Characterization of cross-linking products in $EC F_1$ ATPase. (*A*) $CuCl_2$ induced cross-linking of the ECF_1 from the mutant βY331W:βE381C:ϵS108C. Nucleotide-depleted enzyme (0.2 mg, *lane 2*) was supplemented with 2 mM $MgCl_2$ + 2 mM MgATP for a turnover time of 10 min (MgADP + P_i), followed by the addition and incubation of 75 μM $CuCl_2$ for 1 h at room temperature. The control without $CuCl_2$ is shown in lane 1. (*B*) Cross-linking of wild-type ECF_1 after passage through three centrifuge spin columns. Cross-linked samples were applied to a 10–18% linear gradient of SDS-PAGE and stained with Coomassie blue. The gel was scanned to determine the amount of cross-links. The densitometric analysis was performed using the program ImageQuatNT (Molecular Dynamics, Inc.). The amount of α–δ and β–δ cross-linking products was calculated on the basis of a 1:1 ratio of the two cross-linked products (Grüber and Capaldi, 1996b). Lane 1 corresponds to the untreated enzyme.

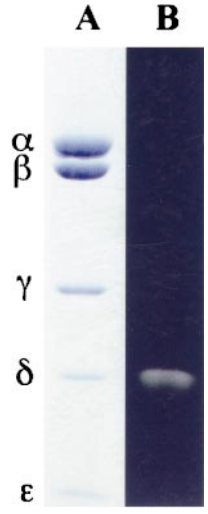

FIGURE 4 Labeling of CM bound at δCys^{140} of wild-type $EC F_1$. The enzyme was reacted with CM as described under Materials and Methods and then subjected to SDS-polyacrylamide gel electrophoresis. (*A*) The gel stained with Coomassie blue; (*B*) the fluorogram of the same gel.

to unambiguously detect such deviations. Therefore, we cannot describe whether all three catalytic sites are filled with saturating concentrations of the nucleotides. It is interesting to note that Weber and Senior (1996, 1997) have shown that three catalytic sites must be occupied for near-maximal ATP hydrolysis activity to be obtained.

Further analysis was done by positioning the known atomic models of the smaller subunits within the low resolution model. The resulting fit to the experimental data with $\chi = 1.68$ (Fig. 1) is higher than that for the low resolution shape. This is not surprising, given that the atomic structures of the γ and δ subunits are only partially available. In all likelihood, the unknown portions of the two subunits would fill the space left in the lower protuberance (Fig. 2) and improve the fit to the experimental data. However, the position of the δ subunit near the bottom of the $\alpha_3\beta_3$ complex and at the interface of an $\alpha\beta$-pair in Fig. 2 is in agreement with the trapped ADP conformation of the $EC F_1$ mutant βY331W:βE381C:ϵS108C with the small subunits linked to β subunits (Grüber and Capaldi, 1996b). As confirmed by the data in Fig. 3 *A*, $CuCl_2$ treatment of this mutant leads to $\beta + \gamma$, $\beta + \epsilon$, $\beta + \delta$, and $\alpha + \delta$ disulfide bond formation. A β-to-δ cross-link product can only be generated if one of the intrinsic Cys residues (Cys^{64}, Cys^{140}) of the elongated δ subunit (Engelbrecht et al., 1991) is in the vicinity of Cys^{381} in the DELSEED-region of the β subunit, suggesting the above position of the δ subunit.

As previously described (Bragg and Hou, 1986; Tozer and Dunn, 1986; Mendel-Hartvig and Capaldi, 1991), an α–δ cross-linked product can be generated in the $EC F_1$ ATPase after the removal of bound nucleotides. The disulfide bond formation, also shown in Fig. 3 *B*, does not occur

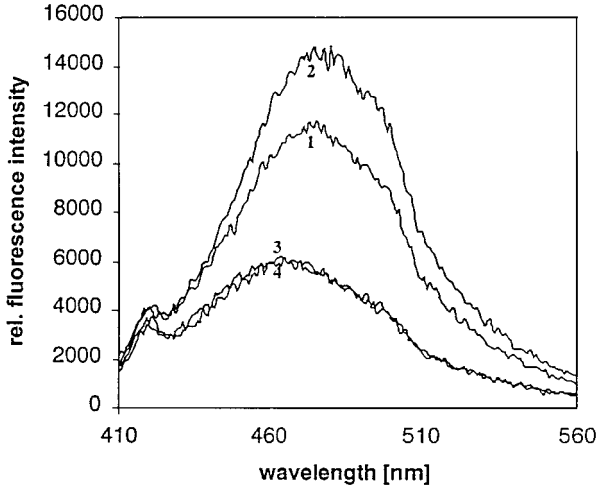

FIGURE 5 Nucleotide induced fluorescence changes of the CM bound $EC F_1$. The emission spectra of wild-type $EC F_1$ were measured with a protein concentration of 100 nM and a 1:1 ratio of MgATP at 12°C. The enzyme was diluted in 50 mM MOPS, at pH 7.5, and 10% glycerol (v/v). *Curve 1*: enzyme in the absence of nucleotides (after three consecutive spin columns); *curve 2*: after addition of 2 mM MgATP, MgAMP · PNP (*curve 3*), or MgADP (*curve 4*) to the $EC F_1$ ATPase. The spectra were recorded 5 min after addition of nucleotide at $\lambda_{ex} = 365.1$ nm with the emission and excitation slits at 5 nm.

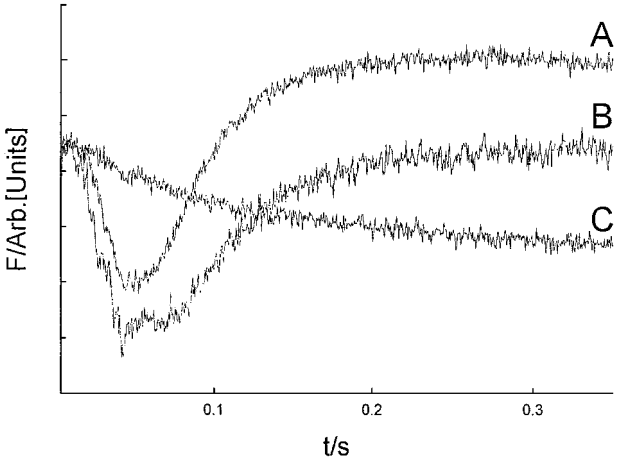

FIGURE 6 Stopped-flow mixing fluorescence transient of *EC*F_1 ATPase, covalently labeled with CM at δCys^{140}. *EC*F_1 ATPase (final concentration 100 nM) was rapidly mixed with an equal volume of a solution containing 2 mM MgATP (final concentration) at 12°C. The excitation and emission wavelengths were 365 nm and 420 nm, respectively. The curves refer to the following nucleotides: A, MgAMP · PNP; B, MgADP; C, MgATP.

after the final step in the purification of the native *EC*F_1 ATPase, where ATP and EDTA are present (Bragg and Hou, 1986) and can also not be generated in the *EC*F_1F_0 complex (Tozer and Dunn, 1986). Recently, a disulfide bond in the *EC*F_1F_0, generated from an α subunit via a cysteine at position 2 to the δ subunit, was described (Ogilvie et al., 1997) but no cross-linking between Cys^2 of the α subunit and the cysteine residues of the δ subunit was obtained for the *EC*F_1 ATPase in these studies. Taken together, these results imply that the α–δ and β–δ cross-links are made possible by a flexibility of the δ subunit in the *EC*F_1 complex associated with nucleotide binding (see below).

The data-fitting procedure is quite sensitive to the positioning of the ϵ subunit. Thus, moving the ϵ subunit by ~0.5 nm from its position in Fig. 2 worsens the χ by ~0.1 which, according to the *F* statistics (Bevington et al., 1969), is statistically significant with a probability of 0.997. The model indicates that the C-terminal domain of the ϵ subunit, consists of two α-helices below the C-terminal domain of the β subunit (Fig. 2). This proximity is confirmed by cross-links between the β and ϵ subunits induced by 1-ethyl-3-[3-(dimethylamino)propyl]carbodiimide (EDC) (Dallmann et al., 1992) or disulfide bond formation between a cysteine inserted at position 381 of the β subunit and a cysteine at position 108 of the ϵ subunit in the presence of ADP [(Aggeler et al., 1995), see also Fig. 3 *A*]. The hydrophobic side chains of the ϵ subunit (Wilkens et al., 1995; Uhlin et al., 1997) face the γ subunit and the perpendicular face of the β-sandwich domain, including residues 31 and 38 of strand β4 (Uhlin et al., 1997), is turned toward the bottom of the enzyme. The ϵ subunit can be disulfide cross-linked with the c subunit of the F_O part (Zhang and Fillingame, 1995).

The most straightforward interpretation of the above cross-linking data for the δ subunit is that there are two structural arrangements and/or conformations in the *EC*F_1 ATPase, one found when nucleotides have been removed and the second one when ADP is present in the catalytic sites. By incorporation of the fluorescent label CM into Cys^{140} of the δ subunit, we found that the fluorescence emission spectrum is sensitive to nucleotides bound in the catalytic sites. The fluorescence enhancement seen on adding MgATP and the fluorescence quenching after addition of MgADP and MgAMP · PNP clearly suggests structural changes in the δ subunit in response to nucleotide binding.

That ATP binding causes conformational changes in the δ subunit is further supported by data for ATP hydrolysis by CM-labeled *EC*F_1 ATPase using the stopped-flow technique. When the enzyme was mixed with MgATP the fluorescence was quenched with a rate constant similar to that measured for ATP hydrolysis. This indicates the structural changes observed in the δ subunit and ATP hydrolysis are linked together. However, it has to be noted that the fluorescence quenching after addition of MgATP following rapid mixing in the stopped-flow experiment (Fig. 6) shows the opposite effect of that observed in the steady-state experiment (Fig. 5). This can be explained in terms of two processes: one producing a fluorescence change within the stopped-flow mixing time, and another one occurring more slowly. The steady-state signal records the total fluorescence change, whereas the stopped-flow transient records only those fluorescence changes occurring after the mixing time. Nucleotide binding will, at these highly saturating concentrations, produce a rapid fluorescence change within the mixing time of the machine, which will be followed by another fluorescence change resulting from the subsequent conformational rearrangement of the δ subunit.

There is evidence that nucleotide binds tightly to one of the noncatalytic sites, with a dissociation constant (K_d) of 1 μM (Matsui et al., 1997). Conformational changes and/or movements of the δ subunit, which is shown to be at the interface (see above), where the noncatalytic sites are located (Abrahams et al., 1994), might be expected to determine the binding affinities of the noncatalytic sites. Such behavior could be studied with appropriate mutants, which should allow one to relate the fluorescence changes observed to kinetically distinct steps in the ATP binding and ATP hydrolysis reaction.

In summary, the low resolution model presented here accounts for the internal structure of the *EC*F_1 ATPase under defined nucleotide conditions. It fits well with the experimental x-ray scattering data, and the relative positioning of the subunits is in good agreement with the cross-linking studies. This should allow further refinements and positioning of the minor subunits γ, δ, and ϵ of trapped conformations within the *EC*F_1 ATPase (Grüber and Capaldi, 1996b). Additionally, the fluorescence and cross-linking results indicate that there are nucleotide-dependent conformational changes and/or rearrangements of the δ sub-

unit, which can be attributed to the flexibility of the δ subunit within the *EC*F_1 ATPase.

The authors are grateful to Gerlinde Brützel for enzyme preparation, Prof. Dr. E. Bamberg (MPI für Biophysik) and Dr. R. J. Clark for their interest and support of this work, and Prof. R. A. Capaldi (University of Oregon, Eugene) for the gift of pGG1 and the strain RA1. D.J.K. acknowledges financial support from the Max-Planck-Gesellschaft. M.B.K is grateful for support from the GKSS Research Center.

This research was supported by the Deutsche Forschungsgemeinschaft (SFB171/B4), by Human Frontiers (HFSP, RG0571/1996-M), and by the International Association for the Promotion of Cooperation with Scientists from the Independent States of the Former Soviet Union (INTAS) Grant 96-1115 (to D.I.S. and M.H.J.K.).

REFERENCES

Abrahams, J. P., A. G. W. Leslie, R. Lutter, and J. E. Walker. 1994. Structure at 2.8 Å resolution of F_1 ATPase from bovine heart mitochondria. *Nature*. 370:621–628.

Aggeler, R., M. A. Haughton, and R. A. Capaldi. 1995. Disulfide bond formation between the COOH-terminal domain of the β subunits and the γ and ε of the *Escherichia coli* F_1 ATPase. *J. Biol. Chem.* 270: 9185–9191.

Aggeler, R., I. Ogilvie, and R. A. Capaldi. 1997. Rotation of a γ-ε subunit domain in the *Escherichia coli* F_1F_O-ATP synthase complex. *J. Biol. Chem.* 272:19621–19624.

Arnold, A., H. U. Wolf, B. P. Ackermann, and H. Bader. 1976. An automated continuous assay of membrane-bound and soluble ATPases and related enzymes. *Anal. Biochem.* 71:209–213.

Bernstein, F. C., T. F. Koetzle, G. J. B. Williams, E. F. Meyer, M. D. Brice, J. R. Rodgers, O. Kennard, T. Shimanouchi, and M. Tasumi. 1977. The Protein Data Bank: a computer-based archival file for macromolecular structures. *J. Mol. Biol*. 112:535–542.

Bevington, P. B. 1969. Data Reduction and Error Analysis for the Physical Sciences. McGraw-Hill, New York.

Bianchet, M., X. Yaern, J. Hullihem, P. L. Pedersen, and M. Amzel. 1991. Mitochondrial ATP synthase-quaternary structure of the F_1 moiety at 3.6 Å determined by X-ray diffraction analysis. *J. Biol. Chem.* 286: 21197–21201.

Boekema, E. J., and B. Böttcher. 1992. The structure of ATP synthase from chloroplasts. Conformational changes of CF_1 studied by electron microscopy. *Biochim. Biophys. Acta*. 1098:131–143.

Boulin, C. J., R. Kempf, A. Gabriel, and M. H. J. Koch. 1988. Data acquisition systems for linear and area X-ray detectors using delay line readout. *Nucl. Instrum. Methods*. A269:312–320.

Boulin, C., R. Kempf, M. H. J. Koch, and S. M. McLaughlin. 1986. Data appraisal, evaluation and display for synchroton radiation experiments: hardware and software. *Nucl. Instrum. Methods*. A249:399–407.

Bragg, P. D., and C. Hou. 1986. Effect of disulfide cross-linking between α and δ subunits on the properties of the F_1 adenosine triphosphate of *Escherichia coli*. *Biochim. Biophys. Acta*. 851:385–394.

Dallmann, H. G., T. G. Flynn, and S. D. Dunn. 1992. Determination of the 1-ethyl-3-[(3-dimethylamino)propyl)]-carbodiimide-induced cross-link between the β and ε subunits of *Escherichia coli* F_1 ATPase. *J. Biol. Chem.* 270:24609–24614.

Deckers-Hebestreit, G., and K. Altendorf. 1996. The F_1F_O-type ATP synthase of bacteria: structure and function of the F_O-complex. *Annu. Rev. Microbiol.* 50:791–824.

Dulley, J. R., and P. Gieve. 1975. A simple technique for eliminating interference by detergents in the Lowry method of protein determination. *Anal. Biochem.* 64:136–147.

Engelbrecht, S., and W. Junge. 1997. ATP synthase, a tentative structural model. *FEBS Lett.* 414:484–491.

Engelbrecht, S., J. Reed, F. Penin, D. C. Gautheron, and W. Junge. 1991. Subunit δ of chloroplast F_OF_1-ATPase and OSCP of mitochondrial F_OF_1-ATPase: a comparison by CD-spectroscopy. *Z. Naturforsch.* 46c: 759–764.

Feigin, L. A., and D. I. Svergun. 1987. Structure Analysis by Small-Angle X-Ray and Neutron Scattering. Plenum, New York.

Fiske, C. H., and Y. Subbarow. 1925. The colorimetric determination of phosphorus. *J. Biol. Chem.* 66:375–400.

Gabriel, A., and F. Dauvergne. 1982. The localization method used at EMBL. *Nucl. Instrum. Methods*. 201:223–224.

Gogol, E. P., R. Aggeler, M. Sagermann, and R. A. Capaldi. 1989b. Cryoelectron microscopy of *Escherichia coli* F_1 adenosinetriphosphatase decorated with monoclonal antibodies to individual subunits of the complex. *Biochemistry*. 28:4717–4724.

Gogol, E. P., U. Lücken, T. Bork, and R. A. Capaldi. 1989a. Molecular architecture of *Escherichia coli* F_1 adenosine triphosphatase. *Biochemistry*. 28:4709–4716.

Grüber, G., and R. A. Capaldi. 1996a. Differentiation of catalytic sites on *Escherichia coli* F_1 ATPase by laser photoactivated labeling with [^{3}H] 2-azido-ATP using the mutant βGlu381Cys:εSer108Cys to identify different β subunits by their interactions. *Biochemistry*. 35:3875–3879.

Grüber, G., and R. A. Capaldi. 1996b. The trapping of different conformations of the *Escherichia coli* F_1 ATPase by disulfide bond formation: effect on nucleotide binding affinities on the catalytic sites. *J. Biol. Chem.* 271:32623–32628.

Grüber, G., A. Hausrath, M. Sagermann, and R. A. Capaldi. 1997. An improved purification of *EC*F_1 and *EC*F_1F_O by using a cytochrome *bo*-deficient strain of *Escherichia coli* facilitates crystallization of these complexes. *FEBS Lett.* 410:165–168.

Koch, M. H. J., and J. Bordas. 1983. X-ray diffraction and scattering on disordered systems using synchroton radiation. *Nucl. Instrum. Methods*. 208:461–469.

Kozin, M. B., V. V. Volkov, and D. I. Svergun. 1997. ASSA—a program for three dimensional rendering in solution scattering from biopolymers. *J. Appl. Crystallogr*. 30:811–815.

Matsui, T., E. Muneyuki, M. Honda, W. S. Allison, C. Dou, and M. Yoshida. 1997. Catalytic activity of the $\alpha_3\beta_3\gamma$ complex of F_1-ATPase without noncatalytic nucleotide binding site. *J. Biol. Chem.* 272: 8215–8221.

Mendel-Hartvig, J., and R. A. Capaldi. 1991. Structure-function relationships of domains of the δ subunit in *Escherichia coli* adenosine triphosphatase. *Biochim. Biophys. Acta*. 1060:115–124.

Ogilvie, I., R. Aggeler, and R. A. Capaldi. 1997. Cross-linking of the δ subunit to one of the three α subunits has no effect on functioning, as expected if δ is a part of the stator that links the F_1 and F_O parts of the *Escherichia coli* ATP synthase. *J. Biol. Chem.* 272:16652–16656.

Schägger, H., and G. von Jagow. 1987. Tricine-sodium dodecyl sulfate-polyacrylamide gel electrophoresis for the separation of proteins in the range from 1 to 100 kDa. *Anal. Biochem.* 166:368–379.

Shirakihara, Y., A. G. W. Leslie, J. P. Abrahams, J. E. Walker, T. Ueda, Y. Sekimoto, M. Kambara, K. Saika, Y. Kagawa, and M. Yoshida. 1997. The crystal structure of the nucleotide-free $\alpha_3\beta_3$ subcomplex of F_1-ATPase from the thermophilic *Bacillus PS3* is a symmetric trimer. *Structure*. 5:825–836.

Stuhrmann, H. B. 1970. Ein neues Verfahren zur Bestimmung der Oberflächenform und der inneren Struktur von gelösten globulären Proteinen aus Röntgenkleinwinkelmessungen. *Zeitschr. Physik. Chem. Neue Folge*. 72:177–198.

Svergun, D. I. 1992. Determination of the regularization parameters in indirect transform methods using perceptual criteria. *J. Appl. Crystallogr*. 25:495–503.

Svergun, D. I. 1993. A direct method of small-angle scattering data treatment. *J. Appl. Crystallogr*. 26:258–267.

Svergun, D. I. 1994. Solution scattering from biopolymers: advanced contrast variation data analysis. *Acta Crystallogr*. A50:391–402.

Svergun, D. I., C. Barberato, and M. H. J. Koch. 1995. CRYSOL—a program to evaluate x-ray solution scattering of biological macromolecules from atomic coordinates. *J. Appl. Crystallogr*. 28:768–773.

Svergun, D. I., C. Barberato, M. H. J. Koch, L. Fetler, and P. Vachette. 1997a. Large differences are observed between the crystal and solution quaternary structures of allosteric aspartate transcarbamylase in the R state. *Proteins*. 27:110–117.

Svergun, D. I., N. Burkhardt, J. Skov Pedersen, M. H. J. Koch, V. V. Volkov, M. B. Kozin, W. Meerwink, H. B. Stuhrmann, G. Diedrich, and K. H. Nierhaus. 1997b. Solution scattering structural analysis of the 70 S *Escherichia coli* ribosome by contrast variation. *J. Mol. Biol.* 271: 588–601, 602–618.

Svergun, D. I., A. V. Semenyuk, and L. A. Feigin. 1988. Small-angle scattering data treatment by the regularization method. *Acta Crystallogr*. A44:244–250.

Svergun, D. I., and H. B. Stuhrmann. 1991. New developments in direct shape determination from small-angle scattering. 1. Theory and model calculations. *Acta Crystallogr*. A47:736–744.

Svergun, D. I., V. V. Volkov, M. B. Kozin, and H. B. Stuhrmann. 1996. New developments in direct shape determination from small-angle scattering. 2. Uniqueness. *Acta Crystallogr*. A52:419–426.

Svergun, D. I., V. V. Volkov, M. B. Kozin, H. B. Stuhrmann, C. Barberato, and M. H. J. Koch. 1997c. Shape determination from solution scattering biopolymers. *J. Appl. Crystallogr*. 30:798–802.

Tozer, R. G., and S. D. Dunn. 1986. Column centrifugation generates an intersubunit disulfide bridge in *Escherichia coli* F_1-ATPase. *Eur. J. Biochem.* 161:513–518.

Turina, P., and R. A. Capaldi. 1994. ATP Hydrolysis-driven structural changes in the γ subunit of *Escherichia coli* ATPase monitored by fluorescence from probes bound at introduced cysteine residues. *J. Biol. Chem.* 272:19621–19624.

Uhlin, U., G. B. Cox, and J. M. Guss. 1997. Crystal structure of the ϵ subunit of the proton-translocating ATP synthase from *Escherichia coli*. *Structure*. 5:1219–1230.

Weber, J., and A. E. Senior. 1996. F_1F_O-ATP synthase: development of direct optical probes of the catalytic mechanism. *Biochim. Biophys. Acta*. 1275:101–104.

Weber, J., and A. E. Senior. 1997. Catalytic mechanism of F_1-ATPase. *Biochim. Biophys. Acta*. 1319:19–58.

Wilkens, S., F. W. Dahlquist, L. P. McIntosh, L. W. Donaldson, and R. A. Capaldi. 1995. Structural features of the ϵ subunit of the *Escherichia coli* ATP synthase determined by NMR spectroscopy. *Nature Struct. Biol.* 2:961–967.

Wilkens, S., S. D. Dunn, J. Chandler, F. W. Dahlquist, and R. A. Capaldi. 1996. Solution structure of the N-terminal domain of the δ subunit of the *E. coli* ATP synthase. *Nature Struct. Biol.* 4:198–201.

Zhang, Y., and R. H. Fillingame. 1995. Subunits coupling H^+ transport and ATP synthesis in the *Escherichia coli* ATP synthase. Cys-Cys cross-linking of F_1 subunit ϵ to the polar loop of F_1 subunit c. *J. Biol. Chem.* 270:24609–24614.

Ziegler, M., R. Xiao, and H. S. Penefsky. 1994. Close proximity of Cys^{64} and Cys^{140} in the δ subunit of *Escherichia coli* F_1-ATPase. *J. Biol. Chem.* 269:4233–4239.